



ELSEVIER

Journal of Molecular Liquids 109 (2004) 83–97

journal of
MOLECULAR
LIQUIDS

www.elsevier.com/locate/molliq

Real and imaginary parts of the vibrational relaxation of acetonitrile in its electrolyte solutions: new results for the dynamics of solvent molecules

Dmitry Nerukh^{a,*}, Trevor R. Griffiths^b^aDepartment of Chemistry, University of Cambridge, Lensfield Road, Cambridge CB2 1EW, UK^bDepartment of Chemistry, University of Leeds, Leeds LS2 9JT, UK

Abstract

Isotropic scattering Raman spectra of liquid acetonitrile (AN) solutions of LiBF₄ and NaI at various temperatures and concentrations have been investigated. For the first time imaginary as well as real parts of the solvent vibrational correlation functions have been extracted from the spectra. Such imaginary parts are currently an important component of modern theories of vibrational relaxation in liquids. This investigation thus provides the first experimental data on imaginary parts of a correlation function in AN solutions. Using the fitting algorithm we recently developed, statistically confident models for the Raman spectra were deduced. The parameters of the band shapes, with an additional correction, of the ν_2 AN vibration (CN stretching), together with their confidence intervals are also reported for the first time. It is shown that three distinct species, with lifetimes greater than $\sim 10^{-13}$ s, of the AN molecules can be detected in solutions containing Li⁺ and Na⁺. These species are attributed to AN molecules directly solvating cations; the single oriented and polarised molecules interleaving the cation and anion of a Solvent Shared Ion Pair (SShIP); and molecules solvating anions. These last are considered to be equivalent to the next layer of solvent molecules, because the CN end of the molecule is distant from the anion and thus less affected by the ionic charge compared with the anion situation. Calculations showed that at the concentrations employed, 1 and 0.3 M, there were essentially no other solvent molecules remaining that could be considered as bulk solvent. Calculations also showed that the internuclear distance in these solutions supported the proposal that the ionic entity dominating in solution was the SShIP, and other evidence was adduced that confirmed the absence of Contact Ion Pairs at these concentrations. The parameters of the shape of the vibrational correlation functions of all three species are reported. The parameters of intramolecular anharmonic coupling between the potential surfaces in AN and the dynamics of the intermolecular environment fluctuations and intermolecular energy transfer are presented. These results will assist investigations made at higher and lower concentrations, when additional species and interactions with AN molecules will be present.

© 2003 Elsevier B.V. All rights reserved.

Keywords: Acetonitrile; Solvation; Vibrational dynamics; Spectra fitting software

1. Introduction

Vibrational spectroscopy has been widely used for studying liquid acetonitrile (AN) [1–8]. These studies have been mainly devoted to the structural properties of pure AN and its solutions in inert solvents but there are reports on the investigations of AN molecules in liquid electrolyte solutions [9–14]. The advantage of studying this molecule is that its vibrational spectra have pronounced, well separated bands attributed to individual vibrations. The spectral bands of commonly used elec-

trolytes that are soluble in AN do not overlap with the solvent bands. The interaction of AN molecules with cations is strong enough to alter significantly the spectrum and produce additional spectral bands [15,16]. These features allow valuable qualitative information concerning the structure and dynamics of the AN electrolyte solutions to be obtained, but when examined quantitatively the results can vary significantly.

There are several reasons for this. First, even though the spectral bands are separated, they often overlap and have a complex inner structure. This means that decomposition into individual spectral bands is required. The set of bands and the models for their shape are different in different studies and thus the parameters obtained are not unique. Second, the resolution procedure is a non-

*Corresponding author. Tel.: +44-1223-763078; fax: +44-1223-763076.

E-mail addresses: dn232@cam.ac.uk (D. Nerukh), t.r.griffiths@chem.leeds.ac.uk (T.R. Griffiths).

linear fitting that must be performed with great care. Failure to choose a statistically correct model or to find a unique solution can lead to erroneous values of the resulting parameters [17]. This is particularly important because the molecular dynamics data or the influence of the electrolyte is contained in the fine detail of the spectrum. Third, the spectral information alone is usually not enough to reconstruct unambiguously the details of microscopic molecular processes in solution. Consequently, the assumptions made about the species present, their lifetimes and other characteristics, and the diversity of these assumptions, produce a range in the final values of the microscopic parameters of AN solutions.

The above shows that the results are very sensitive to the details of the numerical analysis of the experimental spectra. Nevertheless, the spectra do contain much information that, when combined with the data from external sources, may be used to reveal the details of the structure and dynamics of AN electrolyte solutions. The aim of the present study is to extract reliably as much information as possible from the isotropic Raman spectra of LiBF_4 and NaI AN solutions at different temperatures and electrolyte concentrations, focusing on the vibrational dynamics of the solvent molecules. Particular attention has been paid to the fitting procedure and to extracting all possible features from the experimental spectra. We here demonstrate the detection of *three* distinct species of AN molecules from the Raman spectra. In addition, the parameters of the *shape* of both *real and imaginary* parts of the vibrational autocorrelation function, not just the relaxation times, are obtained for the first time.

2. Method

We used a specific procedure for elucidating the theoretical model underlying the experimental spectra. It consisted of a combination of the optimisation runs with analysis of the quality of fit. The optimisation method used was a robust algorithm based on a random search class optimisation method previously shown to be particularly effective in fitting spectral profiles. Full details and applications to various spectra are reported in Ref. [17]. Here we focus on the measures required to choose a correct theoretical model for fitting.

The information, which is implicitly encoded in the theoretical model, is of three kinds. First, the particular function representing a band carries the information concerning the shape of the band. For example, while Lorentz and Gauss functions have the same number of parameters, the information about their shape is obviously different. Second, the values of the adjustable parameters define the spectrum profile. As with the previous example, if two Lorentzian bands have different widths, they represent different band profiles. Third, some parameters of the model can be interrelated. This

is usually the case when the model cannot be further simplified but the values of the parameters still have high confidence intervals. In this situation, it may happen that the ill-defined adjustable parameters are linked by a functional dependence with fixed characteristics. If this is so, expressing some of them through the others can reduce the number of ill-defined parameters.

The steps of the algorithm are as follows:

1. **Input:** a hierarchy of the models; experimental spectrum;
2. Deduce the **statistically correct model:**
 - a choose the simplest model;
 - b fit;
 - c analyse the residuals: if there is a non-random trend—go to 2g (elaborate);
 - d check for the uniqueness of the solution: if it is not unique—go to 2g (simplify);
 - e calculate the confidence intervals for the solution: if it is not confident—go to 2g (simplify);
 - f go to 3;
 - g redefine (choose) the model: simplify (go down in the hierarchy), or elaborate (go up in the hierarchy);
 - h go to 2b;
3. **Output:** structural and dynamical parameters of the liquid.

At step 1 various options for the set of bands and their shapes are introduced as an input. They are organized in a hierarchy so that a model at a specified level of complexity can be chosen. For example, the bands of Gaussian and Lorentzian shapes are at the same level of complexity while the Voigt function (the integral convolution of the two) is at a higher level. If a band is likely to consist of a sum of several simpler bands, various combinations of the primitive type bands can be formed as the alternatives of different complexity. Since we are interested in physically meaningful decompositions, the model should be chosen with the microscopic characteristics of the liquids in mind, i.e. the set of bands should correspond to the possible species and the band shapes should be based on physical models of the correlation functions.

Step 2 is a loop designed to elucidate the particular model from the input. The model is both complex enough to reproduce all the features of the spectrum and at the same time simple enough to provide a unique solution [17]. The criteria for evaluating the appropriateness of the model are represented at steps 2c–2e. The details concerning analysing residuals, checking the uniqueness and calculating the confidence intervals are described in Ref. [17].

The interval of possible values of a parameter is defined by two factors. First, the solution is, strictly speaking, always non-unique. The range in the value of a parameter that keeps the Sum of Squares of Deviations

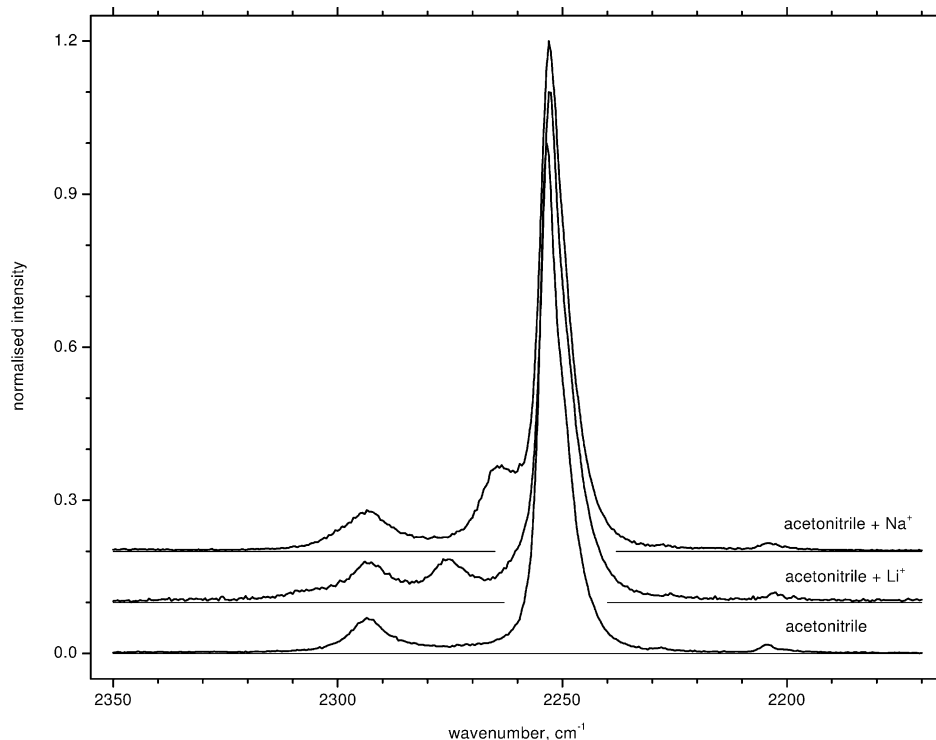


Fig. 1. Isotropic Raman scattering of liquid AN and its 1 M LiBF₄ and NaI solutions at 25 °C.

within the prescribed boundaries [17] defines the confidence interval of the parameter. Second, when a ‘unique’ solution is found, the confidence intervals are calculated using a standard statistical procedure—the Monte Carlo method in our case. This too will produce the confidence interval of the parameter. The greater of the two should be taken as a ‘true’ confidence interval.

The redefinition of the model at step 2g involves adding or removing bands or choosing their shape according to the hierarchy of the models set at step 1. The simplifying procedure depends on the confidence intervals of the parameters. If the interval covers those values of the parameter that makes the whole feature negligible (i.e. the height of the band or the Gaussian width become zero), this parameter is excluded from the model (the whole band is removed or the Voigt function is replaced by a Lorentzian). Conversely, if the effect of the parameters is still non-negligible, its dependence on the other parameters has to be checked and if real, should be introduced. For example, if a function $f(a, b)$ depends on a, b where a and b are ill-defined (have large confidence intervals), the substitution can be made of $f(a, \alpha, \beta)$, where $b = \alpha + \beta a$ and α, β now have small confidence intervals.

After the spectrum has been fitted with an appropriate model, the structural and dynamic characteristics of the liquid can be calculated (step 3). The former includes the number of species in the system, their relative concentration and other static physical parameters. The

latter normally implies the application of the Fourier transformation to the band profiles that provide the correlation functions of the relaxation processes in the liquid.

3. Implementation

This algorithm, together with specific theoretical models, is implemented by the authors in the software package ‘Sp’ (‘Spectra Handler’) [17]. It incorporates an ‘Interpreter’ of maths-like language for describing band profiles. Besides standard profiles such as Lorentzian or Gaussian, the bands can be directly expressed through the correlation functions in time domain. This way of defining the fitting model is very powerful and allows effective implementation of non-trivial models and inter-parameter dependencies. The robust method of fitting provides unique results for very large numbers of fitting parameters: 30, 40 and greater. The package includes the algorithm for calculating confidence intervals using the Monte Carlo method; generating theoretical spectra for testing purposes; and other features. The package can be obtained from Ref. [18].

4. Results and discussion

Typical spectra of AN and its solutions are presented in Fig. 1. Additional bands (shifted to higher wavenumbers) appear in the solution spectra not only next to

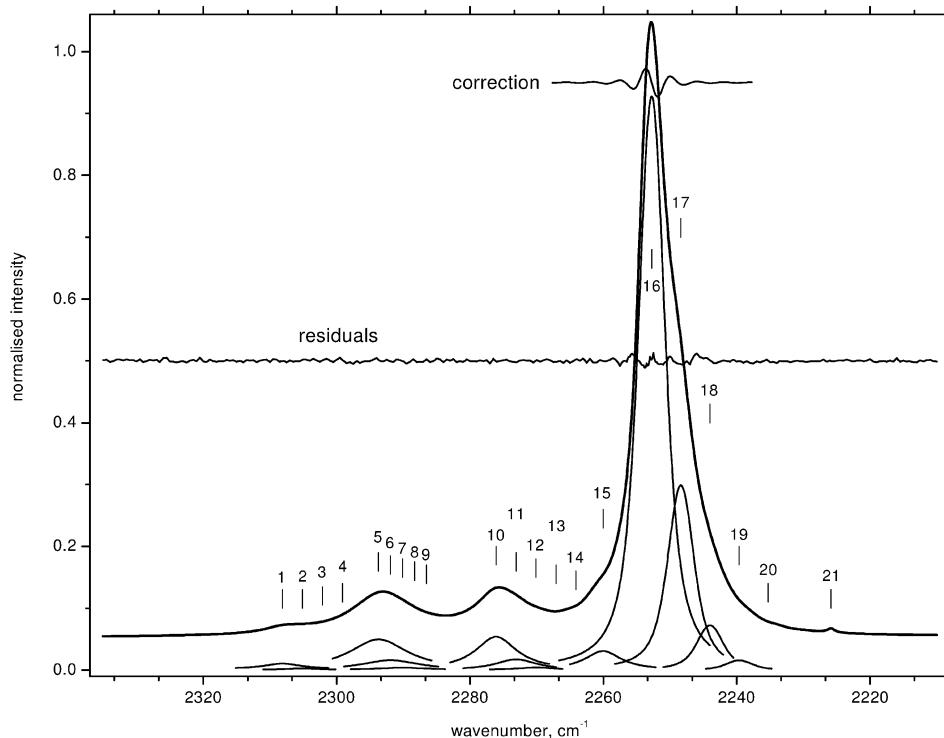


Fig. 2. The set of bands used to decompose the spectrum of isotropic Raman scattering of 1 M LiBF₄ AN solution at 25 °C. The particular model for the bands is given in table 1. The numbers labelling the bands and the meaning of ‘correction’ are explained in the text.

the main ν_2 vibration line ($\sim 2250 \text{ cm}^{-1}$) but also close to the combination $\nu_3 + \nu_4$ mode band ($\sim 2290 \text{ cm}^{-1}$). We have also found similar satellites for the ν_4 vibration band. There are no comparable bands in the spectra of Bu₄NI solution [19] that suggest that these bands are attributed to the AN molecules interacting with the cations Li⁺ and Na⁺. This is because these ions have high positive charge density due to their small size and interact with the negative end of the permanent dipole of the AN molecule, the nitrogen atom. Since the ν_2 vibration mainly involves CN stretching, the assignment of these additional bands is unambiguous. This assignment has been previously reported [15,16].

An example of the resolution of the Li⁺ solution is shown in Fig. 2. Also plotted are the fitting residuals, which are almost completely random. As a basic model of the ν_2 band, the set of the fundamental transition and four ‘hot’ bands was chosen (see Ref. [20] for details). It was found that an asymmetric ‘correction’ [20] was required (also shown in the figure). We define a ‘correction’ f as a (small valued) function that is added to the main band profile and has the property of approaching zero at the band origin and on the wings:

$$I(\nu) = I_0(\nu) + f(\nu - \nu_{\max}), \quad (1)$$

where I is a corrected profile, ν is the wavenumber, I_0 is an original band shape, ν_{\max} is a band position. The

simplest possible form of the correction included two adjustable parameters:

$$f(\nu, S_0^i, \sigma^i) = S_0^i I(\nu - \nu_{\max}) \sin(\sigma^i \nu), \quad (2)$$

where S_0^i and σ^i are the adjustable parameters. The list of bands used for fitting the spectra is as follows:

- the fundamental ν_2 vibration and its ‘hot’ bands: bands 16–20;
- the ν_2 vibration modified by the electrolyte: bands 10–14;
- an additional band modified by the electrolyte: band 15;
- the $\nu_3 + \nu_4$ combination vibration and its ‘hot’ bands: bands 5–9;
- the $\nu_3 + \nu_4$ vibration modified by the electrolyte: bands 1–4;
- some auxiliary small bands: 20, 21.

Profiles of two band types were used, the Lorentz and Voigt functions:

$$S_0 L(\nu, \sigma_L, \nu_m) = \frac{S_0}{\pi} \frac{\sigma_L/2}{(\nu - \nu_m)^2 + (\sigma_L/2)^2}, \quad (3)$$

$$S_0 G(\nu, \sigma_G, \nu_m) = \frac{S_0}{\sqrt{2\pi}\sigma_G} \exp\left[-\frac{1}{2}\left(\frac{\nu - \nu_m}{\sigma_G}\right)^2\right], \quad (4)$$

$$V(\nu, S_0, \sigma_L, \sigma_G, \nu_m) = S_0 \int_{-\infty}^{\infty} L(\nu - \mu, \sigma_L, \nu_m) \times G(\mu, \sigma_G, \nu_m) d\mu, \quad (5)$$

where L is a Lorentzian, G is a Gaussian and V is a Voigt profile, and all other parameters have their usual meaning.

The procedure for finding the appropriate corrections is described in Ref. [20]. The ‘hot’ bands have the same parameters as the fundamental band; their heights are multiplied by the corresponding Boltzmann factors; and they are shifted by $\Delta\nu_h$ from the fundamental band [20].

After applying the above procedure for elucidating the correct model, the specific set of bands and their types were obtained for all spectra. They are schematically shown in table 1 Scheme 1, together with their adjustable parameters. Only adjustable parameters are included in the formulae. If a band depends on more parameters than shown in the Table this means that missing parameters are non-adjustable but instead are expressed through the other parameters in the model. For example, all the parameters of the three hot bands of the $\nu_3 + \nu_4$ vibration modified by the electrolyte (bands 5 in the cell for AN–Li⁺ 1 M system at 25 °C, table 1) are the same as the corresponding parameters of the ν_2 vibrations modified by the electrolyte (band 2). These bands are, therefore, symbolised as 3L(•) in table 1.

Also included in table 1 are the links between the parameters found for the solutions containing Na⁺. The confidence intervals for all α s and β s are very low, which make these links considered as rigid constraints for the adjustable parameters.

The resulting values of the adjustable parameters of interest, together with their confidence intervals, are listed in Tables 2–4. The parameters of the additional band (number 15 in Fig. 2, number 3 in table 1) have confidence intervals low enough to justify the existence of this band even in the case of the Na⁺ solution where it is completely covered by the adjacent bands. The same can be said for the asymmetric corrections for the fundamental band in all the systems studied (table 1).

4.1. Structure of the solutions

The parameters related to the structure of the solutions are the band heights. Since the integral areas of all the band profiles used are unity, the S_0 parameter is a direct measure of the concentration of the species in solution (for the spectral line including ‘hot’ bands, S_0 is multiplied by the sum of corresponding Boltzmann factors).

According to the models elucidated, we can distinguish three different species existing in solution: the main bands at ~ 2250 cm⁻¹; the one shifted significantly (~ 2275 cm⁻¹); and the smallest one in between the others at ~ 2260 cm⁻¹. We mark the corresponding

parameters with the superscripts ‘b’, ‘e’ and ‘s’. The average number of solvent molecules surrounding the cation (n_{AN}) can be calculated from the molar concentration of the electrolyte. Then, from the ratios of the band heights, the fraction of the molecules belonging to each class can be calculated (n_b , n_e and n_s). The resulting values, together with the exact molar concentrations, are summarised in Table 5.

The mere appearance of a separate band ‘s’ indicates that the lifetime of this species is greater than 10^{-13} s, the characteristic time of vibrational spectroscopy at these wavenumbers being 10^{-15} – 10^{-14} s. This is direct evidence of a new ‘long-lived’ species, and here reported for the first time.

To rationalize the microscopic structure of the solutions we present cartoons of the ions surrounded by a number of AN molecules corresponding to the solution concentration (Fig. 3). To do this we first assume that the ions are point charges, arranged as in the sodium chloride crystal lattice, and when we calculate their linear separation for 1 and 0.3 M solutions, we find that the statistical internuclear separation of counter ions is 9.4 Å for 1 M solutions and 14.0 Å for 0.3 M solutions (Fig. 4a and b). This is the maximum distance the ions can be apart, assuming only electrostatic interactions (and before any possible ion pairing). Subtracting the ionic radii of a lithium ion and a tetrafluoroborate anion from this distance gives a maximum distance between these ions for solvent molecules of approximately 6 and 10 Å for 1 and 0.3 M solutions, respectively. These distances are not significantly different if a lithium cation is replaced by a sodium cation. The longest axis of an AN molecule, in the direction of its dipole moment, is approximately 5 Å. Molecules between neighbouring anion and cation charged centres will be oriented and polarised, and in the case of 1 M AN solutions, there can thus only be between counter ions a maximum of *one* AN molecule. This molecule, through electrostatic and ion–dipole interactions, will cause the counter ions to move slightly closer together, filling the available, but small, ‘space’. This type of ion pair is termed a Solvent Shared Ion Pair (SShIP) [21].

When we consider the larger available distance between counter ions in 0.3 M solutions it is just possible, but unlikely, that two oriented and polarised AN molecules could fit in the 10 Å available. However, due to the medium value of the relative permittivity (dielectric constant) of AN, approximately 36, and the mutual attraction of the counter ions, we conclude that the majority of the ion pairs in this solution will be of the SShIP variety: ion pairs with two or more solvent molecules between the charged centres, essentially two ions each surrounded by a monolayer of solvent molecules, are termed solvent separated ion pairs (SSIP). The solvating solvent molecules involved this type of ion pairing can be viewed as essentially behaving in the

Table 1. The models used for fitting the spectra. See text for formulae. Missing parameters indicate that they depend on others and, therefore, are not adjustable.

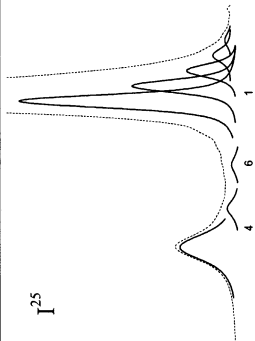
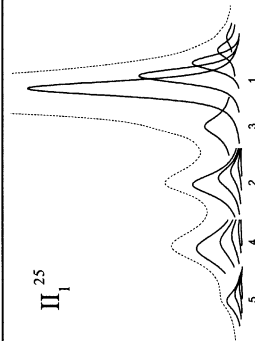
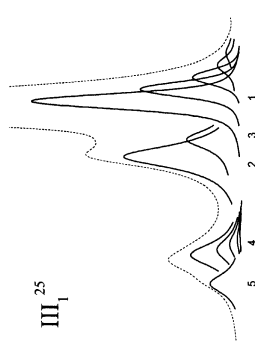
	25°C	50°C	75°C
AN	<p>I_1^{25}</p>  <p>1: $V(S_0^b, \sigma_L^b, \sigma_G^b, v_m^b) + 4V(\Delta v_h^b) + f(S_0^i, \sigma^i)$ 4: $V(S_0^{34}, \sigma_L^{34}, \sigma_G^{34}, v_m^{34}) + L(S_0^b, \sigma^b, v_m^b)$ 6: $L(S_0^b, \sigma^b, v_m^b)$</p>	I_1^{50} Same as I_1^{25}	I_1^{75} Same as I_1^{25}
AN – Li ⁺ 1M	<p>II_1^{25}</p>  <p>1: $V(S_0^b, \sigma_L^b, \sigma_G^b, v_m^b) + 4V(\Delta v_h^b) + f(S_0^i, \sigma^i)$ 2: $L(S_0^e, \sigma^e, v_m^e) + 4L(\Delta v_h^e)$ 3: $L(S_0^s, \sigma^s, v_m^s)$ 4: $L(S_0^{34}, \sigma^{34}, v_m^{34}) + 4L(\Delta v_h^{34})$ 5: $L(\sigma^{e34}, v_m^{e34}) + 3L(\)$</p>	II_1^{50} Same as II_1^{25}	II_1^{75} Same as II_1^{25} , except: 2: $L(S_0^e, \sigma^e, v_m^e)$ 5: $L(\sigma^{e34}, v_m^{e34})$
AN – Li ⁺ 0.3M	<p>$II_{0,3}^{25}$</p> <p>Same as II_1^{25}, except: 2: $L(S_0^e, \sigma^e, v_m^e)$ 5: $L(\sigma^{e34}, v_m^{e34})$</p>	$II_{0,3}^{50}$ Same as II_1^{25} , except: 5: $L(\sigma^{e34}, v_m^{e34})$	$II_{0,3}^{75}$ Same as II_1^{25} , except: 2: $L(S_0^e, \sigma^e, v_m^e)$ 5: $L(\sigma^{e34}, v_m^{e34})$
AN – Na ⁺ 1M	<p>III_1^{25}</p>  <p>links: $S_0^e = \alpha_1^e + \alpha_2^e v_m^e$ $\sigma^e = \beta_1^e + \beta_2^e v_m^e$ $S_0^s = \alpha_1^s + \alpha_2^s \sigma^s$ $v_m^s = \beta_1^s + \beta_2^s \sigma^s$</p>	III_1^{50} Same as III_1^{25}	III_1^{75} Same as III_1^{25}
AN – Na ⁺ 0.3M	<p>$III_{0,3}^{25}$</p> <p>Same as III_1^{25}, except: links: $S_0^e = \alpha_1^e + \alpha_2^e v_m^e$ $\sigma^e = \beta_1^e + \beta_2^e v_m^e$</p>	$III_{0,3}^{50}$ Same as $III_{0,3}^{25}$	$III_{0,3}^{75}$ Same as $III_{0,3}^{25}$

Table 2

Values of the parameters of the ν_2 band of liquid AN at various temperatures. S_0 values are dimensionless, all other parameters have units of cm^{-1}

AN	25 °C		50 °C		75 °C	
S_0^b	5.47	± 0.02 (0.3%)	5.55	± 0.02 (0.3%)	5.58	± 0.06 (1.1%)
σ_L^b	2.50	± 0.05 (2.2%)	2.18	± 0.03 (1.6%)	2.20	± 0.13 (5.9%)
σ_G^b	0.77	± 0.04 (5.1%)	1.13	± 0.02 (1.8%)	1.14	± 0.07 (6.5%)
ν_m^b	2253.27	± 0.007 (0.0%)	2253.49	± 0.004 (0.0%)	2254.19	± 0.00001 (0.0%)
$\Delta\nu_h^b$	4.18	± 0.03 (0.7%)	4.63	± 0.02 (0.4%)	4.52	± 0.05 (1.1%)
S_0^l	0.008	± 0.0005 (5.63%)	0.013	± 0.0003 (2.2%)	0.009	± 0.0008 (8.5%)
σ^l	1.61	± 0.004 (2.44%)	1.51	± 0.01 (1.0%)	1.50	± 0.05 (3.5%)
	Pars: 27		Pars: 27		Pars: 27	

Pars, total number of adjustable parameters. See text for meaning of symbols.

same. The oriented and polarised solvent molecule in the middle of the SShIP can be classed differently.

We now consider the possibility of Contact Ion Pairs in our solutions at the concentrations we have employed. Cartailier et al. [22] have undertaken neutron scattering experiments on 0.68 M LiBr in AN and interpreted their results in terms of the solution containing some anions and cations in contact. In this case, and at this concentration, the smaller size of the bromide ion would have a greater electrostatic attraction for the lithium ion: our solutions contain the much larger tetrafluoroborate anion. Similar studies have been reported by Powell and Nielson [23] for NiCl_2 in methanol. However, the work published by this group, using isotopically pure nickel ions and chloride ions has proposed species in solution that are at variance with traditional interpretations. For example, the number of solvent molecules around nickel has been calculated as close to five, but ligand field spectra, of solutions and hydrated solids, show conclusively that these ions exhibit six solvent ligands in an octahedral arrangement. Thus, until neutron scattering measurements and the calculations therefrom can confirm the authenticated arrangement of solvent molecules around Ni^{2+} then the results of such studies should be treated with caution. In an interesting and relevant study by Griffiths and Wijayanayake [21] on, essentially, the effect of relative permittivity on ion pairing in some 40 solvents, they used the iodides of sodium and tetra-*n*-hexylammonium cations and monitored the sensitive charge transfer to solvent spectrum of the iodide anion. By identifying the characteristic bands and changes with temperature change and other parameters they were able to show that in iodide solutions of no more than 10^{-4} M Contact Ion Pairs were present and dominating only in solvents having relative permittivities less than 5. When the relative permittivity of the solvent was between 5 and 11 the dominant ion pair was the SShIP and between 11 and 23 contains both SShIP and SSIP species. Significantly, they found with AN solutions that with increasing concentration, and thus increasing the competition for the available solvent molecules, the

proportion of first free solvated ions and then SSIP species were reduced to effectively zero and that SSIP dominated. On this basis, and our above interionic calculations, we are confident that the moiety dominating in our AN solutions here is the SShIP. Contact Ion Pairs are thus not considered for the specific AN solutions under study here: from the above calculations for the more concentrated system, if pressed, we would only conclude that the presence and concentration of contact pairs would be but minimal and thus not generate any significantly different AN molecules; certainly Griffiths and Wijayanayake [21] could not generate any evidence for the Contact Ion Pair band that they identified in much lower relative permittivity solvents, even in their highest concentration AN solutions, and upon increasing the temperature to lower their relative permittivity. We also consider that the SShIP is a particularly stable entity because the oriented and polarised solvent molecule in the middle of the SShIP will require considerable energy to remove it.

Considering the ratio of solvent molecules to ions in solution, we can now say that in the 1 M solution there are approximately 20 AN molecules per ion pair (Table 5) and for a 0.3 molar solution, approximately 58 AN molecules (Table 5). This means that, in the former case, there are essentially no ‘bulk’ AN molecules because all these molecules are either located directly next to the ions and solvent molecule comprising the SShIP, solvating this species, or they are involved in providing a subsequent monolayer around this species. For 0.3 M solutions, with a greater average separation between counter ions, this still means that the great majority of the AN molecules will be influenced by the electric field of the ions, as just described.

However, by investigating the CN stretch of AN molecules we can extend the earlier work [21] and consider the difference in the solvation of anions and cations. With the negative end of the molecular dipole, the cyanide end of the AN molecule, oriented towards a cation the vibrations of this group will be much more affected than when this group is oriented away from,

Table 3

Values of the parameters of the ν_2 band for AN–LiBF₄ solutions in AN at various temperatures

AN–Li ⁺ 1 M	25 °C		50 °C		75 °C	
‘b’ band:						
S_0^b	6.08	±0.05 (0.8%)	6.09	±0.05 (0.9%)	5.94	±0.10 (1.5%)
σ_L^b	3.08	±0.12 (3.8%)	2.67	±0.14 (5.1%)	2.19	±0.16 (9.0%)
σ_G^b	0.78	±0.08 (10.5%)	1.12	±0.08 (6.9%)	1.40	±0.07 (3.3%)
ν_m^b	2252.74	±0.15 (0.0%)	2253.16	±0.13 (0.0%)	2253.57	±0.03 (0.0%)
$\Delta\nu_h^b$	4.37	±0.06 (1.3%)	4.84	±0.05 (1.1%)	5.05	±0.09 (1.5%)
S_0^I	0.0043	±0.0008 (19.6%)	0.0085	±0.0008 (8.9%)	0.0098	±0.001 (6.5%)
σ^I	1.59	±0.10 (6.2%)	1.47	±0.05 (3.4%)	1.46	±0.04 (3.5%)
‘e’ band:						
S_0^e	0.64	±0.05 (8.3%)	0.72	±0.06 (8.1%)	1.02	±0.15 (8.1%)
σ^e	7.44	±0.86 (11.5%)	8.75	±1.34 (15.3%)	9.47	±2.83 (31.9%)
ν_m^e	2276.09	±0.25 (0.01%)	2276.08	±0.43 (0.02%)	2274.93	±0.41 (0.02%)
$\Delta\nu_h^e$	3.13	±0.7 (22.7%)	2.41	±1.65 (68.3%)		
‘s’ band:						
S_0^s	0.32	±0.07 (23.5%)	0.55	±0.11 (20.6%)	0.67	±0.21 (53.6%)
σ^s	6.50	±1.57 (24.2%)	8.93	±2.04 (22.8%)	10.97	±3.00 (34.1%)
ν_m^s	2260.04	±0.16 (0.01%)	2261.25	±0.25 (0.01%)	2261.77	±0.24 (0.01%)
	Pars: 31		Pars: 31		Pars: 31	
AN–Li⁺ 0.3 M						
‘b’ band:						
S_0^b	5.66	±0.04 (0.8%)	5.70	±0.04 (0.7%)	5.93	±0.27 (4.5%)
σ_L^b	2.88	±0.09 (3.0%)	2.25	±0.07 (3.8%)	1.80	±1.09 (60.6%)
σ_G^b	0.60	±0.06 (10.6%)	1.18	±0.03 (2.0%)	1.79	±0.55 (30.7%)
ν_m^b	2252.95	±0.009 (0.0%)	2253.12	±0.02 (0.0%)	2253.05	±0.13 (0.01%)
$\Delta\nu_h^b$	4.17	±0.04 (1.1%)	4.68	±0.07 (1.4%)	5.62	±0.45 (8.0%)
S_0^I	0.0067	±0.0006 (9.6%)	0.0106	±0.0008 (5.3%)	0.0128	±0.004 (32.5%)
σ^I	1.63	±0.06 (3.8%)	1.53	±0.04 (2.6%)	1.28	±0.19 (14.4%)
‘e’ band:						
S_0^e	0.49	±0.08 (15.7%)	0.47	±0.09 (17.0%)	0.47	±0.35 (74.4%)
σ^e	11.98	±1.7 (14.4%)	9.34	±2.33 (24.4%)	7.79	±6.3 (81.5%)
ν_m^e	2275.26	±0.06 (0.02%)	2275.38	±0.06 (0.02%)	2277.71	±1.28 (0.06%)
$\Delta\nu_h^e$	7.60	±6.03 (79.5%)	6.86	±1.85 (22.6%)		
‘s’ band:						
S_0^s	0.15	±0.06 (41.8%)	0.10	±0.04 (36.4%)	0.47	±0.41 (85.8%)
σ^s	6.54	±3.3 (50.2%)	3.46	±1.51 (35.9%)	8.77	±3.99 (45.5%)
ν_m^s	2260.03	±0.28 (0.02%)	2260.14	±0.05 (0.02%)	2262.99	±3.19 (0.14%)
	Pars: 30		Pars: 31		Pars: 24	

Pars, total number of adjustable parameters. See text for meaning of symbols. S_0 values are dimensionless, all other parameters have units of cm^{-1} .

and thus farther away from an anion. Further, with the much larger anion, and hence its much smaller charge density per unit area, the tetrafluoroborate ion will have a much smaller effect upon these solvating molecules. Consequently, the CN vibrations will permit a distinction between AN molecules contiguous with cations and those contiguous with anions, the vibrations for these latter now being little different from those expected for the remaining surrounding AN molecules. We can, therefore, identify AN molecules in largely three different locations around ions in both the 1 and 0.3 M solutions investigated here such that the CN vibrations will respond differently.

We assign the ‘e’ band to AN molecules in the first solvation shell of the cation and the ‘s’ band to the AN molecules situated between the ions in SSHIPs (Fig. 4c). We attribute band ‘b’, least affected by the presence of added electrolyte, to the remainder of the AN molecules in solution. These are the ones solvating the anions and their next nearest neighbours. Although differences in the solvation of cations and anions can be distinguished from analysis of the CN vibrations, it is not at present or hereby possible to distinguish between weakly solvating and their next nearest neighbours by Raman spectra alone. This is consistent with the general concept that large anions are weakly solvated or have very low

Table 4
Values of the parameters of the ν_2 band for AN–NaI solutions in acetonitrile at various temperature

AN–Na ⁺ 1 M	25 °C		50 °C		75 °C	
'b' band:						
S_0^b	5.95	±0.02 (0.3%)	6.38	±0.01 (0.2%)	6.33	±0.05 (0.8%)
σ_L^b	2.60	±0.03 (1.1%)	2.73	±0.02 (0.7%)	2.18	±0.11 (5.0%)
σ_G^b	1.16	±0.01 (1.2%)	1.30	±0.01 (0.9%)	1.56	±0.05 (3.5%)
ν_m^b	2252.88	±0.008 (0.0%)	2253.43	±0.008 (0.0%)	2253.98	±0.02 (0.0%)
$\Delta\nu_h^b$	4.11	±0.02 (0.5%)	4.51	±0.01 (0.4%)	4.87	±0.05 (1.1%)
S_0^l	0.0035	±0.0003 (9.9%)	0.0040	±0.0003 (6.8%)	0.0062	±0.0007 (11.1%)
σ^l	1.46	±0.06 (3.8%)	1.41	±0.04 (3.0%)	1.35	±0.10 (7.5%)
'e' band:						
S_0^e	1.42	±0.08 (5.3%)	1.52	±0.06 (3.8%)	1.48	±0.26 (17.3%)
σ^e	7.61	±0.28 (3.7%)	8.27	±0.21 (2.6%)	10.2	±1.12 (11.1%)
ν_m^e	2265.09	±0.21 (0.01%)	2265.53	±0.20 (0.01%)	2265.22	±0.21 (0.01%)
's' band:						
S_0^s	0.65	±0.06 (9.5%)	0.49	±0.05 (9.9%)	0.20	±0.15 (74.9%)
σ^s	7.21	±0.95 (13.2%)	6.34	±0.95 (15.0%)	3.80	±0.53 (13.9%)
ν_m^s	2260.59	±0.24 (0.01%)	2261.25	±0.19 (0.01%)	2261.35	±0.53 (0.02%)
	Pars: 34		Pars: 34		Pars: 34	
AN–Na ⁺ 0.3 M						
'b' band:						
S_0^b	5.72	±0.01 (0.2%)	5.90	±0.05 (0.8%)	5.97	±0.04 (0.7%)
σ_L^b	2.69	±0.02 (0.7%)	2.13	±0.13 (6.3%)	1.74	±0.08 (4.7%)
σ_G^b	0.85	±0.01 (1.7%)	1.34	±0.07 (5.2%)	1.62	±0.04 (2.5%)
ν_m^b	2253.17	±0.07 (0.0%)	2253.30	±0.02 (0.0%)	2253.52	±0.02 (0.0%)
$\Delta\nu_h^b$	4.07	±0.02 (0.6%)	4.69	±0.07 (1.4%)	4.97	±0.05 (1.1%)
S_0^l	0.0058	±0.0004 (6.1%)	0.0096	±0.0009 (8.9%)	0.0087	±0.0007 (8.5%)
σ^l	1.64	±0.04 (2.5%)	1.31	±0.07 (5.2%)	1.38	±0.06 (4.6%)
'e' band:						
S_0^e	0.55	±0.07 (12.5%)	0.84	±0.23 (27.2%)	0.81	±0.24 (29.4%)
σ^e	9.46	±0.81 (8.6%)	11.5	±2.50 (21.7%)	11.3	±2.19 (19.3%)
ν_m^e	2265.40	±0.11 (0.00%)	2264.22	±0.37 (0.02%)	2265.46	±0.07 (0.0%)
's' band:						
S_0^s	0.11	±0.02 (18.2%)	0.12	±0.08 (66.6%)	0.22	±0.006 (2.7%)
σ^s	6.93	±0.49 (7.07%)	5.95	±2.02 (33.9%)	5.00	±0.005 (0.0%)
ν_m^s	2260.82	±0.38 (0.02%)	2260.10	±0.66 (0.03%)	2260.47	±0.03 (0.0%)
	Pars: 32		Pars: 31		Pars: 32	

Pars, total number of adjustable parameters. See text for meaning of symbols. S_0 values dimensionless, all others parameters have units of cm^{-1} .

solvation numbers, though we note that this concept is but rarely considered as a function of concentration and not in the more realistic terms of available interionic distances as we have done above.

While we can be confident that the concentrations chosen for our two solutions are such that Contact Ion Pairs are not present, we do now need to consider other possible entities and interactions. The intensity of spectral bands is generally related to the concentration of the species from which it arises. For our model to be self-contained and at the same time to be able to explain the relative heights of the spectral bands we thus need to consider that not all ions are involved in SShIPs. As we have noted above, there are 'excess' solvent molecules not involved in the contiguous solvation of the

SShIPs. Consequently, we can anticipate that at times molecular collisions will displace an ion from the SShIP to liberate a solvated ion or form a SSIP. These collisions will not have sufficient energy to displace the more firmly held and protected 'oriented and polarised' molecule, our solvent species 's', within the SShIP, on the basis that Contact Ion Pairs are not found at the concentrations in our solutions. Thus, our solutions are dominated by SShIPs but will contain some fraction of 'non-associated' ions, the cations influencing the CN vibration more than the anions, for the reasons given above.

Accordingly, if we consider the Li-containing system, the solution contains k_a SShIP moieties, k_{Li} cations, their ratio is α ; and each cation takes x_{Li} molecules of the

Table 5

The number of AN molecules belonging to different species in the various solutions (n_i) and the molar concentration of these solutions (c_i)

		25 °C	50 °C	75 °C
AN–Li ⁺ 1 M	n_{AN}	19.3	n_b 16.89	16.37 16.38
	c_{Li^+} , M	0.93	n_e 1.78	1.93 1.76
				n_s 0.63
AN–Li ⁺ 0.3 M	n_{AN}	57.5	n_b 53.25	52.55 52.31
	c_{Li^+} , M	0.32	n_e 3.25	4.33 2.59
				n_s 0.99
AN–Na ⁺ 1 M	n_{AN}	19.7	n_b 15.85	16.32 16.93
	c_{Na^+} , M	0.94	n_e 2.66	2.58 2.47
				n_s 1.22
AN–Na ⁺ 0.3 M	n_{AN}	59.0	n_b 54.52	53.20 53.21
	c_{Na^+} , M	0.32	n_e 3.69	5.03 4.51
				n_s 0.74

solvent, and each moiety takes x_a molecules; and there are n_r molecules not belonging to either cation or moiety, then from the following set of equations

$$\left\{ \begin{array}{l} x_{Li}k_{Li} + x_a k_a + n_r = n_{AN}(k_{Li} + k_a) \\ \frac{n_r}{x_{Li}k_{Li}} = \frac{n_b}{n_e} \\ \frac{n_r}{x_a k_a} = \frac{n_b}{n_s} \\ \frac{k_a}{k_{Li}} = a \end{array} \right. \quad (6)$$

the number of AN molecules solvating each cation and moiety, respectively, can be obtained:

$$x_{Li} = n_e(1 + a), \quad (7)$$

$$x_a = n_s \left(1 + \frac{1}{a} \right). \quad (8)$$

Excluding a from these two equations, the relation between x_{Li} and x_a becomes

$$x_a = \frac{n_s}{1 - \frac{n_e}{x_{Li}}} \quad (9)$$

This gives us an important relationship between the numbers of AN molecules solvating cations and moieties

molecules. To illustrate these numbers for the solutions under study we plot both x_{Li} and x_a against a (Fig. 5) for Li⁺ solution (Na⁺ solutions show a similar picture). Note that x_a depends on n_s , which has lower confidence intervals than n_e , and this makes the lines corresponding to x_a in Fig. 5 less reliable than those for x_{Li} .

The main feature of these graphs is a very weak dependence of the 1 M solution parameters on temperature. This can be associated with tight packing of the molecules around ions, which constrains them in the electric field of the ion and thus exceeds the available thermal energy. These graphs also indicate a small number for the interleaving molecules of the SShIP, in agreement with our description of this moiety. Considering the number of AN molecules that can pack around the cations, this should be in the range 5–7 for Li⁺ and somewhat higher for Na⁺ (Fig. 3). These graphs are thus consistent with our interionic calculations that give us less than 2 molecules per SShIP and a high ratio of ion pair formation from below 2 to 3 for 1 M solutions and 0.5 to 1.2 for 0.3 M solutions. The lower association ratio for 0.3 M solutions is still in agreement with the assumption of SShIP formation since the latter should have a lower ratio for more dilute solutions, and this is when somewhat fewer ion pairs are expected.

4.2. Intramolecular potential

The magnitude of the shift of the ‘hot’ bands provides the characteristics of the anharmonic coupling between

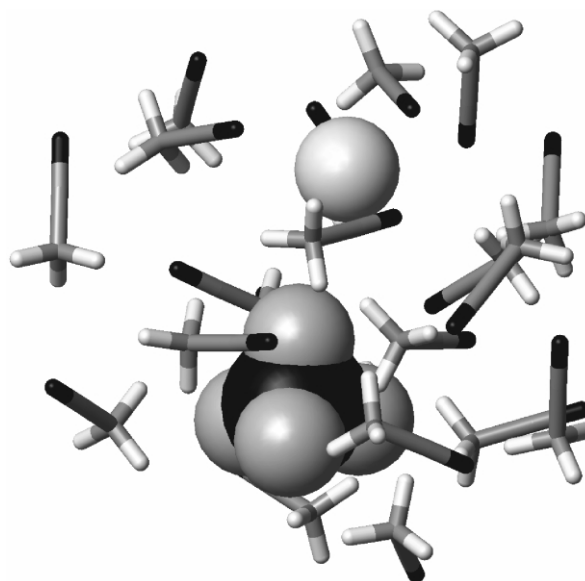


Fig. 3. Cartoon depicting the arrangements of the ions Li⁺ and BF₄⁻ and AN molecules for 1 M solution (19 AN molecule per ion pair) with the Van der Waals radii of the ions shown. The picture was generated using CHEM3D PRO from CHEMOFFICE 2002, 7.0 by CambridgeSoft; the coordinates of the molecules have been optimised by minimising the energy of the cluster. This picture shows that essentially all the solvent molecules, if not contiguous with an ion, are contiguous with the directly solvating molecules.

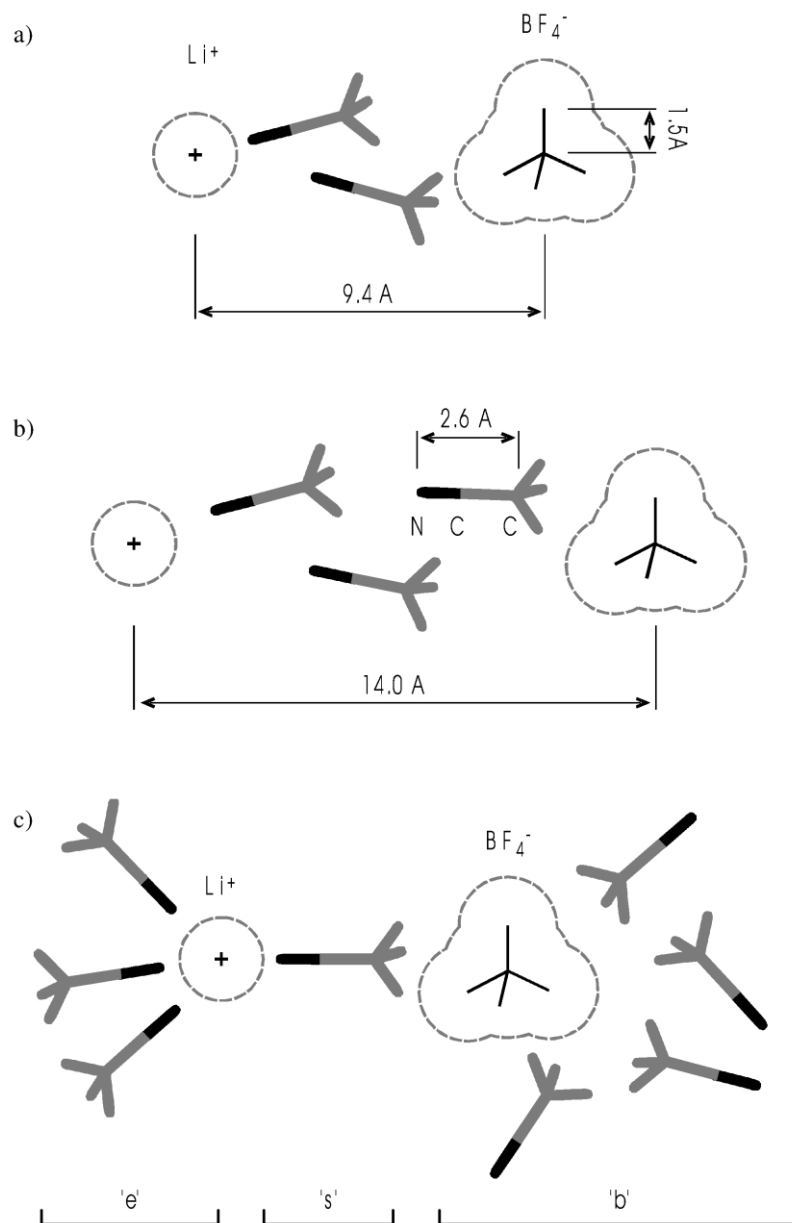


Fig. 4. The three possible types of AN molecules that can be attributed to the species detected in the present study. The cartoons depict the *maximum* statistical distances possible between counter ions in 1 M AN solution, (a) and 0.3 M solution, (b), and the size of AN molecules. The distances and the bond lengths are drawn *to scale*. (c) Shows the major species present in solution, a SSHP, and the orientation of the solvent molecules contiguous with this moiety. The single layer of solvent molecules that surround this moiety, and comprise almost all the remaining solvent molecules in solution, are not shown: the features of their CN vibrations are essentially indistinguishable from those designated 'b'. The radii have Van der Waals values but radii values determined by others will not alter the conclusions here.

the ground and excited potential surfaces of the AN molecule. The frequencies of the 'hot' bands can be expressed as

$$\nu_i[\nu_j] = \nu_i + (g_i + 1)x_{ij}\nu_i + \sum_{j \neq i} x_{ij}\nu_j, \quad (10)$$

where $\nu_i[\nu_j]$ is the frequency of a 'hot' band originating from the state ν_j (1 for the first 'hot' band, 2 for the second and so on), ν_i is a fundamental frequency, g_i is a degeneracy of normal mode i and x_{ij} is an anharmonic

coupling coefficient [24]. Thus, the 'hot' bands shift $\Delta\nu_h$ depends on several anharmonic coupling constants and characterises the details of intramolecular potential surface interactions.

The ν_4 vibrational mode of AN has been investigated [25] and it was shown that the asymmetry of the band is due to the progression of the 'hot' bands. Detailed information about the 'hot' bands in liquid isotopomers of nitromethane is given by Hill et al. [26] where the validity of the same bandwidth for the 'hot' bands as for the fundamental transition is justified. The impor-

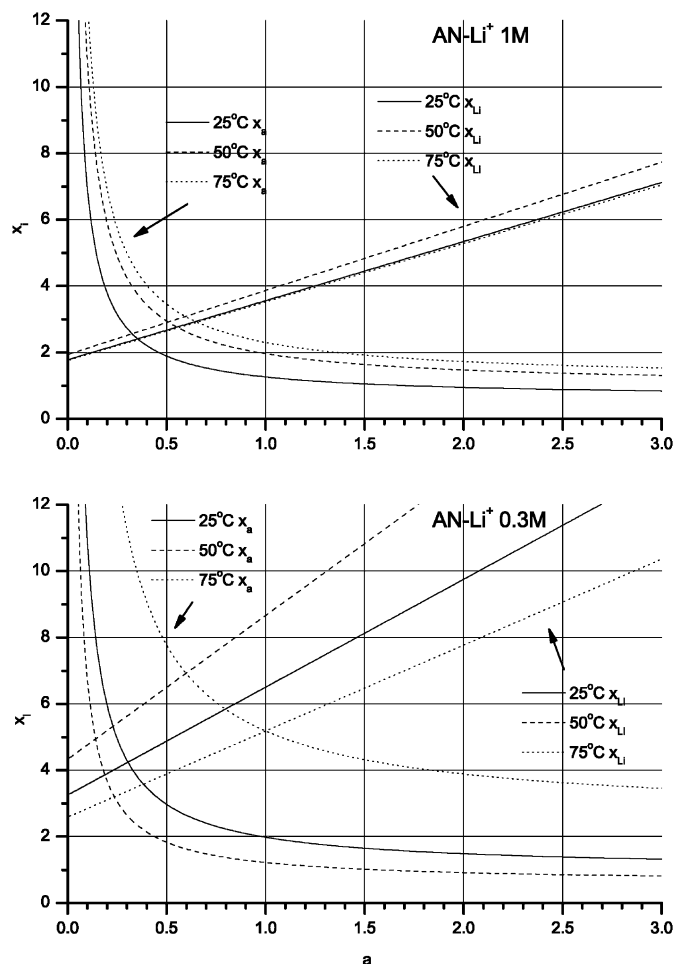


Fig. 5. Dependence of the number of solvating AN molecules x_i on the constant of association a (see text for details).

tance of taking proper account of the ‘hot’ bands for the vibrational spectra of liquids has also been demonstrated [27].

Our results (Tables 3 and 4) show that $\Delta\nu_h$ substantially depends on temperature, and increases with temperature increase. Also, the electrolyte influences this parameter, increasing its value with increase in the number of solvated Li^+ cations. For the remaining AN molecules there is an increase in $\Delta\nu_h$ with concentration and temperature increase in Li^+ -containing solutions, but almost no change in the Na^+ system. The much smaller Li^+ ion has a much greater effect on contiguous solvent molecules than any other alkali metal ion.

4.3. Band positions

The change in the vibrational peak positions in liquids compared with the gas phase value is attributed to the details of intermolecular interactions [28]. In the framework of the theory by Bratos and Tarjus [28] the intermolecular interaction of the active molecules can be represented by the random fluctuations of the envi-

ronment and resonant energy transfer between the active molecules. The shift of the vibrational band with respect to the gas phase is given by

$$\delta\nu = N\hbar\langle\Omega_{12}\rangle + \hbar\langle\Omega_{11}\rangle, \quad (11)$$

where $\hbar\langle\Omega_{11}\rangle$ is a term representing the environment fluctuations of the vibrational frequency and $N\hbar\langle\Omega_{12}\rangle$ represents the resonant transfer of the vibrational energy [28]. We have calculated these shifts for our systems (Table 6). Obviously, the environment fluctuations are changed dramatically in the ion field. This is true both for cations (bands ‘e’ and ‘s’) and anions (‘b’ band). A detailed analysis of the values reported in Table 6 requires an extensive examination of the theory enunciated by Bratos and Tarjus [28] and is beyond the scope of the present paper. However, some preliminary observations can be made.

First, an average trend in the increase in shift values with temperature can be seen. In addition, for the ‘b’ molecules we can conclude that for 0.3 M solutions this increase is slower than that for pure AN and the 1 M

Table 6

The shifts of the peak positions (in cm^{-1}) associated with the three different species of AN molecule in the systems studied

		25 °C	50 °C	75 °C
AN	$\delta\nu_b$	-13.43	-13.21	-12.51
AN-Li ⁺ 1 M	$\delta\nu_b$	-13.96	-13.54	-13.13
	$\delta\nu_e$	9.39	9.38	8.23
	$\delta\nu_s$	-6.66	-5.45	-4.93
AN-Li ⁺ 0.3 M	$\delta\nu_b$	-13.75	-13.58	-13.65
	$\delta\nu_e$	8.56	8.68	11.01
	$\delta\nu_s$	-6.67	-6.56	-3.71
AN-Na ⁺ 1 M	$\delta\nu_b$	-13.82	-13.27	-12.72
	$\delta\nu_e$	-1.61	-1.17	-1.48
	$\delta\nu_s$	-6.11	-5.45	-5.35
AN-Na ⁺ 0.3 M	$\delta\nu_b$	-13.53	-13.4	-13.18
	$\delta\nu_e$	-1.3	-2.48	-1.24
	$\delta\nu_s$	-5.88	-6.6	-6.23

solution. This is because 'b' type molecules are a mixture of molecules, mainly solvating anions and a small quantity of 'bulk' molecules, from which they cannot be distinguished here.

Second, we note that the shifts for the 's' molecules are similar for all solutions, whereas the shifts for 'e' molecules differ for Na⁺ and Li⁺-containing solutions. This supports our conclusion that 's' molecules are the interleaving molecules in the SShIP moieties.

4.4. Vibrational dynamics

Since the spectral bands consist of purely symmetric and purely asymmetric parts, the real and imaginary parts of the corresponding vibrational correlation functions can be obtained [20]. The real part of the vibrational correlation functions of the systems studied is shown in Fig. 6. The relaxation times of the real and imaginary parts of the function are listed in Table 7, as well as the ratios of the Lorentzian and Gaussian components.

The vibrational relaxation in the electrolyte solutions is much faster than in pure AN. The molecules in the ion pair exhibit slightly higher values of vibrational relaxation than that solvating the free cations. The Lorentzian/Gaussian ratio is noticeably higher in the Li⁺ solutions than in the Na⁺ solutions. In all cases, this ratio shows a decrease with increasing temperature.

Direct comparison of the vibrational relaxation times of the 'e' molecules, in the Li⁺ and Na⁺ solutions, is not possible at this time because different models were used to fit the spectra.

Even though the value of the imaginary part of the vibrational dynamics is small it is, nevertheless, not negligible. Interestingly, in all systems it increases with temperature increase.

The dynamic data reported here can be regarded as the experimental values because the models employed

for spectra resolution are general and virtually all possible information has been extracted from the experimental isotropic Raman scattering spectra. This is, we believe, the first report on the vibrational correlation function in its complex form as well as the parameters of the dynamics of 's' molecules, the interleaving molecules in SShIPs.

5. Experimental

Acetonitrile was distilled four times, initially twice from P₂O₅, then from K₂CO₃ before final distillation. The salts were prepared by the repeated recrystallisation from acetone and careful drying under vacuum. Raman spectra were measured using 0.5 cm^{-1} data point intervals on a Ramanor U-1000 spectrometer (Jobin Yvon)

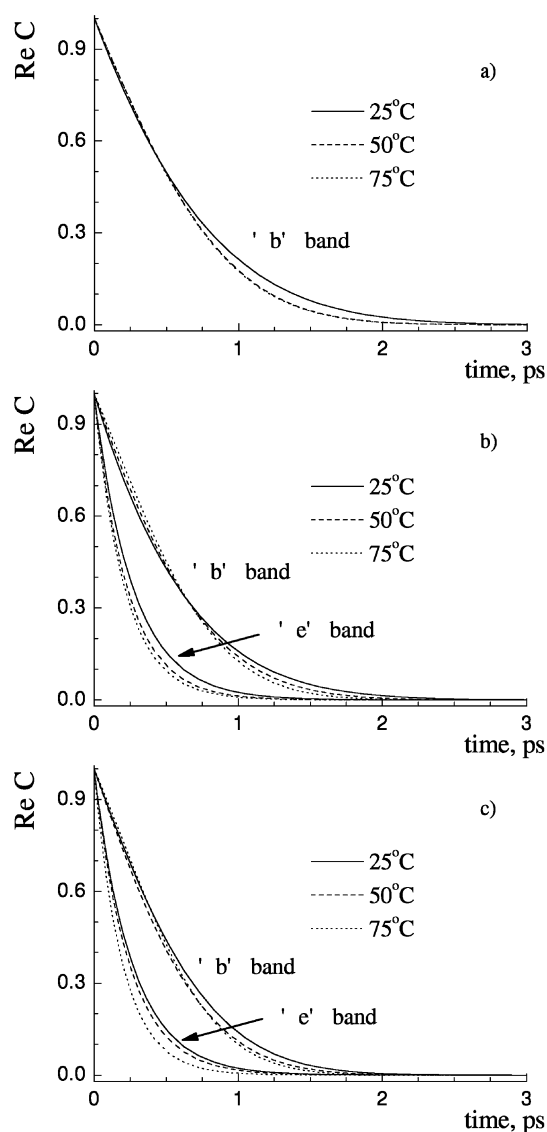


Fig. 6. Real part of the vibrational correlation functions for (a), pure AN; (b), AN-Li⁺ 1 M solution; and (c), AN-Na⁺ 1 M solution.

Table 7

Vibrational relaxation times (in ps) and the ratio of Lorentz and Gauss components of the bands widths of the AN ν_2 vibrations in the systems studied

		25 °C	50 °C	75 °C
AN	τ_r^b	0.64	0.59	0.59
	τ_i^b	-1.48×10^{-3}	-2.49×10^{-3}	-1.78×10^{-3}
	$\sigma[\sigma_L/\sigma_G]^b$	3.25	1.93	1.93
AN–Li ⁺ 1 M	τ_r^b	0.545	0.531	0.528
	τ_i^b	-0.66×10^{-3}	-1.39×10^{-3}	-1.75×10^{-3}
	$[\sigma_L/\sigma_G]^b$	3.95	2.38	1.56
	τ_r^e	0.27	0.23	0.21
	τ_r^s	0.31	0.22	0.18
AN–Li ⁺ 0.3 M	τ_r^b	0.610	0.570	0.489
	τ_i^b	-1.11×10^{-3}	-1.95×10^{-3}	-2.33×10^{-3}
	$[\sigma_L/\sigma_G]^b$	4.8	1.91	1.01
	τ_r^e	0.17	0.21	0.26
	τ_r^s	0.31	0.58	0.23
AN–Na ⁺ 1 M	τ_r^b	0.531	0.491	0.497
	τ_i^b	-0.58×10^{-3}	-0.62×10^{-3}	-1.07×10^{-3}
	$[\sigma_L/\sigma_G]^b$	2.24	2.1	1.40
	τ_r^e	0.26	0.24	0.20
	τ_r^s	0.28	0.32	0.53
AN–Na ⁺ 0.3 M	τ_r^b	0.585	0.547	0.528
	τ_i^b	-0.99×10^{-3}	-1.76×10^{-3}	-1.69×10^{-3}
	$[\sigma_L/\sigma_G]^b$	3.16	1.59	1.07
	τ_r^e	0.21	0.17	0.18
	τ_r^s	0.29	0.34	0.40

τ_r is the real part, τ_i is the imaginary part.

with a resolution of 0.15 cm^{-1} . Further details are given in Refs. [17,19,29].

6. Conclusions

We have demonstrated that, when a statistically rigorous procedure for the resolution of spectra is used, significant and detailed information can be extracted from experimental vibrational spectra. For the first time, the existence of at least three species of AN molecules with lifetimes greater than 10^{-13} s has been shown.

It is important to note that the concentrations we have used, 1 and 0.3 M, represent the concentration range, for the salts employed, for which the dominant species in solution is the SSHIP. This has somewhat simplified our resolution of the Raman spectra into their component bands, and the determination of the vibrational dynamics of the three different species of AN species. With higher concentrations, and thus with reducing internuclear distances, Contact Ion Pairs will appear; and at lower concentrations, below 0.3 M, the proportion of SSHIP and free ions will increase. In addition, the majority of the solvent molecules in dilute solutions will now no longer be involved in either solvating the ions or undergoing dipole–dipole interactions with the molecules contiguous with ions, and consequently these molecules can be better described as bulk molecules.

Thus, we only claim that the three species of AN molecules identified here relate to the 0.3–1.0 M concentration range. Outside this range there will be AN molecules interacting extensively with Contact Ion Pairs, in and with SSHIP, with free ions, and as bulk molecules. The Raman spectra obtained for concentrations outside our experimental range will thus contain additional bands and their resolution will perhaps be more difficult. However, since this study has identified and allocated the bands of three distinct species, future investigations should benefit.

Further, the parameters of the vibrational dynamics of these molecules have been obtained, including the imaginary parts of the vibrational correlation function and its shape. This is the first report providing evidence of the imaginary part of vibrational relaxation in liquid electrolyte solution, and thus new information and experimental values regarding vibrational relaxation has been obtained. The temperature and electrolyte concentration dependence of these parameters are also given here.

Further development must also include a detailed investigation of the modern theories of intermolecular dynamics in liquids and electrolyte solutions, and which employ the imaginary parts of the vibration correlation function. The parameters reported here can thereby open up an experimental basis for checking and developing these theories.

Acknowledgments

The authors thank Serge Eremenko, University of Groningen, The Netherlands, for assistance in obtaining the experimental data and processing the spectra.

References

- [1] S. Hashimoto, T. Ohba, S. Ikawa, *Chem. Phys.* 138 (1989) 63–69.
- [2] B. Guillot, P. Marteau, J. Obriot, *J. Chem. Phys.* 93 (1990) 6148–6164.
- [3] P.O. Westlund, R.M. Lynden-Bell, *Mol. Phys.* 60 (1987) 1189–1209.
- [4] A. Morresi, P. Sassi, M. Paolantoni, S. Santini, R.S. Cataliotti, *Chem. Phys.* 254 (2000) 337–347.
- [5] A. Morresi, P. Sassi, M. Ombelli, G. Paliani, R.S. Cataliotti, *Phys. Chem. Chem. Phys.* 2 (2000) 2857–2861.
- [6] E. Guardia, R. Pinzon, *J. Mol. Liq.* 85 (2000) 33–44.
- [7] C. Breuillar-Alliot, J. Soussen-Jacob, *Mol. Phys.* 28 (1974) 905–1044.
- [8] D. Jamroz, J. Stangret, J. Lindgren, *J. Am. Chem. Soc.* 114 (1993) 6165–6177.
- [9] J.S. Loring, W.R. Fawcett, *J. Phys. Chem. A* 103 (1999) 3608–3617.
- [10] T.G. Chang, D.E. Irish, *J. Solution Chem.* 3 (1974) 161–170.
- [11] V.B. Borisova, V.V. Markelov, S.K. Akopyan, A.M. Shevyakov, N.G. Bakhshiev, *Russ. J. Chem. Phys.* 53 (1979) 215–223.
- [12] M.I.S. Sastry, S. Singh, *Curr. Sci.* 55 (1986) 1157–1166.
- [13] J. Barthel, R. Deser, *J. Solution Chem.* 23 (1994) 1133–1146.
- [14] J. Barthel, *J. Mol. Liq.* 65/66 (1995) 177–185.
- [15] W.R. Fawcett, G. Liu, A.A. Kloss, *J. Chem. Soc. Faraday Trans. 90* (1994) 2697–2701.
- [16] B. Izdebska, Z. Kecki, *Rocz. Chem.* 52 (1978) 1531–1539.
- [17] T.R. Griffiths, D.A. Nerukh, A. Eremenko, *Phys. Chem. Chem. Phys.* 1 (1999) 3199–3208.
- [18] Available from <http://www.chem.pwf.cam.ac.uk/~dn232/software/>.
- [19] D.A. Nerukh, Interparticle interactions and dynamics of molecules in electrolyte solutions of *n*-hexanol and acetonitrile by vibrational spectroscopy, Ph.D. thesis, Kharkov, 1996.
- [20] D. Nerukh, T.R. Griffiths, *Phys. Chem. Chem. Phys.* 3 (2001) 1799–1805.
- [21] T.R. Griffiths, R.H. Wijayanayake, *Trans. Faraday Soc.* 66 (1970) 1563–1573.
- [22] T. Cartailier, W. Kunz, P. Turq, M.-C. Bellissent-Funel, *J. Phys.: Condens. Matter* 3 (1991) 9511–9520.
- [23] D.H. Powell, G.W. Neilson, *J. Phys.: Condens. Matter* 2 (1990) 5867–5876.
- [24] A.V. Nowak, J.L. Lyman, *J. Quant. Spectrosc. Radiat. Transfer* 15 (1975) 945–952.
- [25] R.S. Cataliotti, L. Mariani, A. Morresi, G. Paliani, M.G. Giorgini, *J. Mol. Struct.* 293 (1993) 223–226.
- [26] J.R. Hill, D.S. Moore, S.C. Schmidt, C.B. Storm, *J. Phys. Chem.* 95 (1991) 3037–3044.
- [27] D.S. Moore, *J. Phys. Chem. A* 105 (2001) 4660–4663.
- [28] S. Bratos, G. Tarjus, *Phys. Rev. A* 24 (1981) 1591–1600.
- [29] S.A. Eremenko, O.N. Kalugin, D.A. Nerukh, *Proc. Kharkov Univ. Chem.* 1 (1997) 34–43.